BRAIN CONNECTIVITY
Volume 8, Number 6, 2018

DOI: 10.1089/brain.2017.0558

Alteration of Diffusion-Tensor Magnetic Resonance Imaging Measures in Brain Regions Involved in Early Stages of Parkinson's Disease

Nan-Kuei Chen,[1–6] Ying-Hui Chou,[3,7,8] Mark Sundman,[7] Patrick Hickey,[9] Willard S. Kasoff,[10,11] Adam Bernstein,[1] Theodore P. Trouard,[1,2,6,12] Tanya Lin,[11,13] Steven Z. Rapcsak,[11] Scott J. Sherman,[11] and Carol P. Weingarten[4,14]

Abstract

Many nonmotor symptoms (e.g., hyposmia) appear years before the cardinal motor features of Parkinson's disease (PD). It is thus desirable to be able to use noninvasive brain imaging methods, such as magnetic resonance imaging (MRI), to detect brain abnormalities in early PD stages. Among the MRI modalities, diffusion-tensor imaging (DTI) is suitable for detecting changes in brain tissue structure due to neurological diseases. The main purpose of this study was to investigate whether DTI signals measured from brain regions involved in early stages of PD differ from those of healthy controls. To answer this question, we analyzed whole-brain DTI data of 30 early-stage PD patients and 30 controls using improved region of interest-based analysis methods. Results showed that (i) the fractional anisotropy (FA) values in the olfactory tract (connected with the olfactory bulb: one of the first structures affected by PD) are lower in PD patients than healthy controls; (ii) FA values are higher in PD patients than healthy controls in the following brain regions: corticospinal tract, cingulum (near hippocampus), and superior longitudinal fasciculus (temporal part). Experimental results suggest that the tissue property, measured by FA, in olfactory regions is structurally modulated by PD with a mechanism that is different from other brain regions.

Keywords: diffusion-tensor imaging; olfactory tract; Parkinson's disease

Introduction

Parkinson's Disease (PD) is the second most common neurodegenerative disorder. Diagnosis of PD is often delayed far into the disease course, and current treatments fail to modify disease progression. At the time of clinical diagnosis, 60–70% of dopaminergic neurons may already be damaged. This may have hampered the successful translation to clinical trials of many neuroprotective treatments that appear effective in animal models. Thus, early diagnosis and objective measures of disease progression are of utmost importance in developing disease modifying therapies.

Many nonmotor symptoms, such as hyposmia, pain sensation, rapid eye movement sleep behavior disorder, and constipation, appear years before the cardinal motor features of PD, making them attractive early biomarkers particularly if there were objective and quantifiable measures available. As discussed by Braak and colleagues (2004), PD in Braak's stages 1 and 2 mainly affects olfactory bulb, olfactory nucleus, dorsal motor nucleus of the vagus in the medulla oblongata, and pontine tegmentum (Braak et al., 2004; Del Tredici and Braak, 2016; Goedert et al., 2013). Identification of prodromal abnormalities in these brain regions for individual patients would greatly facilitate the development of novel

Departments of [1]Biomedical Engineering and [2]Medical Imaging, University of Arizona, Tucson, Arizona.
[3]Arizona Center on Aging, University of Arizona, Tucson, Arizona.
[4]Brain Imaging and Analysis Center and [5]Department of Radiology, Duke University Medical Center, Durham, North Carolina.
[6]BIO5 Institute and [7]Department of Psychology, University of Arizona, Tucson, Arizona.
[8]Cognitive Science Program, University of Arizona, Tucson, Arizona.
[9]Department of Neurology, Kaiser Permanente, Los Angeles, California.
[10]Division of Neurosurgery, Department of Surgery and [11]Department of Neurology, University of Arizona, Tucson, Arizona.
[12]Evelyn F McKnight Brain Institute, University of Arizona, Tucson, Arizona.
[13]Department of Neurology, Southern Arizona VA Health Care System, Tucson, Arizona.
[14]Department of Psychiatry and Behavioral Sciences, Duke University Medical Center, Durham, North Carolina.

diagnostic and interventional approaches that could be applied at the earliest stages of neurodegeneration.

Diffusion-tensor imaging (DTI), a magnetic resonance imaging (MRI) method designed to characterize water diffusion properties, is suitable for detecting changes in brain tissue structure due to neurological diseases (Basser et al., 1994; Pierpaoli et al., 1996). Brain tissue pathology may be reflected in one or more of the following DTI-derived measures: (i) fractional anisotropy (FA: the degree of anisotropy of water diffusion), (ii) axial diffusivity (AD: the water diffusivity along the primary eigenvector direction, along the axis of the axon in white matter), (iii) radial diffusivity (RD: the water diffusivity perpendicular to the primary eigenvector direction, perpendicular to the axis of the axon in white matter), and (iv) mean diffusivity (MD: the mean water diffusivity along all directions).

Recently, DTI has been successfully applied to detect PD-induced brain tissue abnormalities in multiple gray- and white-matter regions. Three meta-analyses of DTI studies on PD have been published to date (Atkinson-Clement et al., 2017; Cochrane and Ebmeier, 2013; Schwarz et al., 2013). Two of the studies focused on the substantia nigra, a hallmark structure whose degradation is linked to motor symptoms of PD (Cochrane and Ebmeier, 2013; Schwarz et al., 2013). A third meta-analysis assessed subcortical, cortical, white-matter, and cerebellar regions, and observed significant alterations in PD in many regions, including the substantia nigra, caudate, putamen, globus pallidus, olfactory cortex, and white matter of the corpus callosum and corticospinal tracts (Atkinson-Clement et al., 2017). In most existing studies, DTI measures were obtained from PD patients in Braak's stage 3 or higher. As a result, the reported findings, which might reflect the combination of PD pathology, medication effects, and neural compensatory mechanisms at later PD stages, are not highly consistent. For example, (i) DTI measures of the substantia nigra have been variable with respect to whether significant differences exist between PD patients and healthy controls (Atkinson-Clement et al., 2017; Schwarz et al., 2013; Wen et al., 2016), and (ii) Mole and associates (2016) observed FA increase in some brain regions (e.g., corticospinal tract) and FA decrease in other regions (e.g., uncinate fasiculus) in PD patients, suggesting that tissue in different brain regions may be structurally modulated by PD with distinct pathological (or compensatory) mechanisms.

In 2010, Ibarretxe-Bilbao and colleagues observed FA differences in the olfactory tract between early-stage PD patients and controls based on tract-based spatial statistics (TBSS) analysis of DTI data (Smith et al., 2006), implying that DTI signal abnormalities reflecting pathological processes in early PD stages may be clinically detectable. A potential concern regarding this study is that the chosen TBSS method could be overconservative, and thus potentially susceptible to false negatives due to the nature of voxel-based analyses or residual image misalignment across the subjects. For these reasons, in a more recent TBSS-based study, Georgiopoulos and colleagues (2017) observed only AD difference, but no FA difference, in the olfactory tract between PD and controls. In studies performed by Rolheiser and associates (2011) and Joshi and colleagues (2017), the authors measured DTI signals from two sets of regions of interest (ROIs; olfactory region and substantia nigra), and found that the DTI signals of olfactory regions could better differentiate early-stage PD patients from healthy controls when compared with signals from the substantia nigra. These issues may be better addressed using advanced diffusion weighted imaging (DWI) processing pipelines, which were recently developed based on machine learning (Kim and Park 2016) or tractometry analysis (Cousineau et al., 2017).

The purpose of this study was to use an improved DTI processing method to assess group differences between PD patients and healthy controls in nonmotor brain regions implicated in early stages of PD according to Braak's hypothesis. As discussed above, this question may not have been adequately answered in existing studies that were limited in two ways: First, TBSS-based studies to date were potentially susceptible to false negatives. Second, other previous ROI-based studies of the olfactory system included only a small set of ROIs (Georgiopoulos et al., 2017; Joshi et al., 2017; Rolheiser et al., 2011). In this study, we analyzed whole-brain DTI data obtained from 30 PD patients (Hoehn and Yahr scales 1 and 2 in 25 patients) and 30 healthy controls using an improved ROI analysis procedure. The chosen ROIs were based on Mori's Johns Hopkins University white-matter tractography atlas (Wakana et al., 2007), which was made available through Oxford Centre for Functional MRI Software Library (FSL; see https://fsl.fmrib.ox.ac.uk/fsl/fslwiki/Atlases). Two additional sets of ROIs, covering substantia nigra and olfactory tracts (not part of Mori's atlas), were added to this study.

Methods

Participants

All research involving human participants was approved by the Institutional Review Board of Duke University Medical Center. Written and oral informed consents were obtained from all the participants.

DTI data were obtained from 30 healthy controls (16 females; 28 right-handed) and 30 PD patients (7 females; 26 right-handed). Most PD patients were in early stages (Hoehn and Yahr scales between 1 and 2 for 25 patients). Inclusion criteria for subjects were as follows: (i) between 40 and 85 years of age, (ii) male or female, and (iii) healthy volunteers or subjects diagnosed with PD. Exclusion criteria were as follows: (i) MRI contraindications and claustrophobia; (ii) severe or unstable medical disorders or conditions, drugs that may cause depression, or any condition that in the investigators' opinions made the patient unsuitable for participating in the study (e.g., clinically significant cirrhosis); (iii) any of the following—lifetime history of alcohol or substance dependence, schizophrenia or other psychotic disorder, bipolar disorder, psychotic features of depression, or current (last 6 months) obsessive–compulsive disorder or panic disorder; in general, subjects with a history of other Axis I disorders before their depression were excluded; (iv) active suicidality or current suicidal risk as determined by the investigator; (v) significant handicaps (e.g., visual or hearing loss, mental retardation) that would interfere with neuropsychological testing or the ability to follow study procedures; (vi) known primary neurological disorders (such as tumors, multiple sclerosis, and seizure disorder) other than PD; (vii) Mini Mental State Examination (MMSE) of <25; and (viii) any other factor that in the investigators' judgment may affect patient safety or compliance.

Table 1. Demographic and Behavioral Measures of Participants

	PD patients (mean ± standard deviation)	*Healthy controls (mean ± standard deviation)*	*p*
Age	64.03 ± 10.30	58.03 ± 9.28	0.022
Gender	7 females	15 females	0.032
Education	17.2 ± 2.83	16.77 ± 2.19	0.51
MMSE	29.68 ± 0.85	29.73 ± 0.58	0.82
UPDRS III	17.93 ± 9.72	0.33 ± 0.96	<0.000001
Hoehn and Yahr[a]	1.74 ± 0.85	0 ± 0	<0.000001
Months since diagnosis	62.9 ± 43.6 (min: 1; max: 162)		
Predominant side of motor symptoms	15 left; 15 right		

[a]Twenty-five PD patients had Hoehn and Yahr scales between 1 and 2; one patient had Hoehn and Yahr scale 2.5; two patients had Hoehn and Yahr scale 3; two patients had Hoehn and Yahr scale 4.

PD, Parkinson's disease; MMSE, Mini Mental State Examination; UPDRS, Unified Parkinson's Disease Rating Scale.

Among the 30 PD patients, 18 underwent two scan sessions: on and off medication. The following behavioral and clinical measures were obtained from the participants: (i) Unified Parkinson's Disease Rating Scale (UPDRS), (ii) Hoehn and Yahr Stage, (iii) Beck Depression Inventory (BDI-II), and (iv) MMSE. In this study, we only analyzed MRI data obtained during ''on medication'' sessions. Table 1 summarizes the demographic and clinical data of the two groups.

MRI data acquisition

MRI data were acquired with a 3 T MRI scanner (General Electric Healthcare, Waukesha), equipped with an eight-channel radio frequency (RF) coil, at Duke University Medical Center. DTI data were acquired with a single-shot dual-refocused spin-echo parallel echo-planar imaging pulse sequence with the following scan parameters: field of view (FOV) = 23 cm × 23 cm; in-plane matrix size = 128 × 128; parallel imaging acceleration factor = 2; echo time (TE) = 80 msec; repetition time (TR) = 8 sec; sagittal-plane slice thickness = 1.8 mm; voxel size = 1.8 mm^3; number of slices = 78; $b = 1000$ sec/mm^2; number of diffusion-encoding directions = 25; and number of repetitions = 2. These DTI scan parameters were suitable for imaging major white-matter tracts, including the olfactory tract (Skorpil et al., 2011).

DTI data preprocessing

The acquired data were processed with the following steps: Step 1: the images were effectively denoised using our recently developed diffusion-matched principal component analysis based two-channel denoising procedure (Chen et al., 2018). Step 2: the eddy current-induced distortions and image misalignment due to head motion were corrected with FSL (https://fsl.fmrib.ox.ac.uk) (Andersson and Sotiropoulos, 2016). Step 3: FA maps were then reconstructed with FSL. Step 4: FA maps from all the subjects were registered to a common space using the skeleton-based normalization provided by FSL-TBSS (https://fsl.fmrib.ox.ac.uk/fsl/fslwiki/TBSS) (Smith et al., 2006). In this study, the TBSS was only used to align FA maps to a common space, and the aligned images (without being skeletonized) were further analyzed with an ROI-based analysis described in the next section.

DTI-derived measures from ROIs

The following 13 ROIs were included in our analyses: olfactory tract, substantia nigra, anterior thalamic radiation, corticospinal tract, cingulum (cingulate gyrus), cingulum (hippocampus), forceps major, forceps minor, inferior fronto-occipital fasciculus, inferior longitudinal fasciculus, superior longitudinal fasciculus, uncinate fasciculus, and superior longitudinal fasciculus. Eleven of these ROIs were defined by Mori's Johns Hopkins University white-matter tractography atlas, and two ROIs (olfactory tract and substantia nigra) were manually drawn by an author (N.-K.C.).

The mean FA value for an ROI was calculated from each of the participants bilaterally. That is, the mean FA values were computed using ROIs from both hemispheres, without differentiating left versus right hemispheric results or taking the predominant side of motor symptoms into consideration, for the following reasons: First, the ultimate goal of this study is to produce a DTI measure that is capable of detecting brain signal abnormalities before the onset of unilateral PD motor symptoms. Therefore, we were more interested in assessing the detectability of PD-related brain abnormalities using DTI signals from both hemispheres. Second, Joshi and associates (2017) reported that the FA differences in olfactory tract between PD and controls were not associated with the primary side of motor symptoms among PD patients. Therefore, motor symptom lateralization was not considered in the current analyses.

Statistical analyses

For each of the ROIs, we performed the unequal variance *t*-tests to examine the difference in FA values between PD patients and healthy controls. Because of potential confounding effects of gender and age, these two variables were regressed out with linear regression. Multiple comparisons (from 13 ROIs) were addressed with Bonferroni correction when examining the significance of group differences (i.e., corrected p threshold = 0.05/13 = 0.0038).

Results

The two-tailed *t*-tests yielded group effects on FA values for the olfactory tract (uncorrected $p = 0.0054$; effect size = 0.75; controls > PD), corticospinal tract (uncorrected $p = 0.0041$; effect size = 0.77; PD > controls), cingulum: near hippocampus (uncorrected $p = 0.0030$; effect size = 0.80; PD > controls), inferior longitudinal fasciculus (uncorrected $p = 0.0341$; effect size = 0.56; PD > controls), uncinate fasciculus (uncorrected $p = 0.0411$; effect size = 0.54; PD > controls), and superior longitudinal fasciculus: temporal

Table 2. Region of Interest-Based Fractional Anisotropy Measures of Parkinson's Disease Patients and Healthy Controls

	PD patients (mean ± standard deviation)	*Healthy controls (mean ± standard deviation)*	*Two-sided p-value*	*Effect size*
Olfactory tract: 4188 voxels	0.118 ± 0.012	0.129 ± 0.017	0.0054**	**0.75**
Substantia nigra: 192 voxels	0.385 ± 0.027	0.395 ± 0.027	0.134	0.38
Anterior thalamic radiation: 16,720 voxels	0.319 ± 0.026	0.317 ± 0.018	0.789	0.07
Corticospinal tract: 10,739 voxels	0.498 ± 0.026	0.475 ± 0.033	0.0041**	**0.77**
Cingulum (cingulate gyrus): 2877 voxels	0.430 ± 0.040	0.419 ± 0.040	0.240	0.30
Cingulum (hippocampus): 1355 voxels	0.353 ± 0.025	0.334 ± 0.024	0.0030*	**0.80**
Forceps major: 6458 voxels	0.478 ± 0.029	0.476 ± 0.020	0.700	0.09
Forceps minor: 19,407 voxels	0.346 ± 0.022	0.342 ± 0.018	0.353	0.24
Inferior fronto-occipital fasciculus: 12,751 voxels	0.376 ± 0.022	0.370 ± 0.020	0.220	0.32
Inferior longitudinal fasciculus: 9551 voxels	0.383 ± 0.023	0.371 ± 0.019	0.034	0.56
Superior longitudinal fasciculus: 17,657 voxels	0.326 ± 0.026	0.321 ± 0.018	0.376	0.23
Uncinate fasciculus: 1985 voxels	0.330 ± 0.020	0.320 ± 0.017	0.041	0.54
Superior longitudinal fasciculus (temporal part): 374 voxels	0.451 ± 0.028	0.424 ± 0.038	0.0033*	**0.79**

Effect size >0.75 in bold.
*Statistically significant after multiple comparison correction ($p < 0.0038$: two tailed).
**The corrected p-value is slightly larger than our threshold (0.0038: two tailed).

part (uncorrected $p = 0.0033$; effect size = 0.79; PD > controls). Two of these ROIs, superior longitudinal fasciculus (temporal part) and cingulum (near hippocampus), demonstrated significant group difference in FA values with Bonferroni correction ($p < 0.0038$). FA values in two other ROIs, including olfactory tract and corticospinal tract, demonstrated group difference with effect size >0.75 and with their p-values slightly larger than the Bonferroni-corrected p-value threshold. Among all of these ROIs, only the olfactory tract demonstrated lower FA values in PD when compared with healthy controls. In agreement with the findings reported by Mole and colleagues (2016), the FA values in many ROIs are higher in PD patients than in healthy controls. The results of t-tests are summarized in Table 2, and the locations of four ROIs (olfactory tract, corticospinal tract, superior longitudinal fasciculus: temporal part, and cingulum: near hippocampus) are shown in Figure 1.

The FA values (in the chosen ROIs) are negatively correlated with the UPDRS III scores across PD patients, as shown in Table 3, in which signals from the cingulum (cingulate gyrus) demonstrate one-tailed statistical significance after multiple comparisons. In contrast, the correlation between

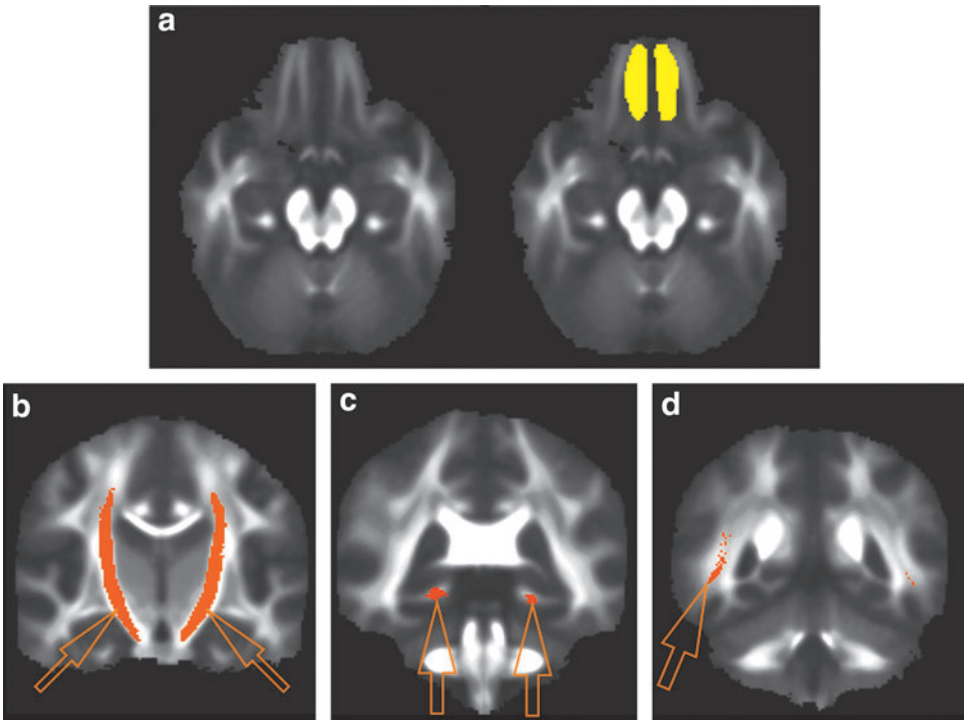

FIG. 1. **(a)** The mean fractional anisotropy map (of a chosen axial slice: left panel) and the manually drawn olfactory tract region of interest (ROI; in yellow: right panel). **(b)** The corticospinal tract ROI (indicated by arrows) from Mori's Johns Hopkins University white-matter tractography atlas. **(c)** The cingulum (near hippocampus: indicated by arrows) ROI from Mori's Johns Hopkins University white-matter tractography atlas. **(d)** The superior longitudinal fasciculus (temporal part) ROI from Mori's Johns Hopkins University white-matter tractography atlas. Only the right side of ROI is shown in this coronal slice in **(d)**. Color images available online at www.liebertpub.com/brain

Table 3. Correlation Between Fractional Anisotropy Values and Unified Parkinson's Disease Rating Scale III and Disease Duration Across Parkinson's Disease Patients

	UPDRS III	*Disease duration*
Olfactory tract	−0.245	0.003
Substantia nigra	−0.460**	0.176
Anterior thalamic radiation	−0.414**	0.090
Corticospinal tract	−0.254	−0.273
Cingulum (cingulate gyrus)	−0.480*	0.077
Cingulum (hippocampus)	−0.440**	0.026
Forceps major	−0.450**	0.018
Forceps minor	−0.380**	0.010
Inferior fronto-occipital fasciculus	−0.343**	0.051
Inferior longitudinal fasciculus	−0.285	−0.037
Superior longitudinal fasciculus	−0.371**	−0.023
Uncinate fasciculus	−0.360**	−0.166
Superior longitudinal fasciculus (temporal part)	−0.282	−0.153

*Statistically significant with multiple comparison correction ($p < 0.0038$: one tailed).

**Significant without multiple comparison correction ($p < 0.05$: one tailed).

FA values and disease duration patients is neither as uniform nor as significant across 13 ROIs (Table 3).

Discussion

This study produced the following knowledge: First, after examining the DTI-derived measures from 13 ROIs, we found that FA values are lower in PD patients than in healthy controls in the olfactory tract, which is connected with the olfactory bulb: one of the first structures affected by PD. Second, the FA values are higher in PD patients than in controls in several other brain regions, including corticospinal tract, in agreement with the findings by Mole and associates (2016); and superior longitudinal fasciculus (temporal part), and cingulum (near hippocampus). Our data strongly suggest that the tissue structural properties measured by FA in the olfactory regions (where FA of controls > FA of PD) are modulated by PD with a different mechanism when compared with other brain regions (where FA of PD > FA of controls), such as neurodegenerative versus compensatory mechanisms. The results from our study also suggest that the FA measures obtained from these brain regions may potentially be used to detect brain signal changes in an early stage of PD, possibly even before the clinical manifestation of motor symptoms. This remains to be confirmed by future studies.

In addition to olfactory bulb and olfactory nucleus, brain regions involved in Braak's stages 1 and 2 of PD include medulla oblongata and pontine tegmentum (Braak et al., 2004). In this study, we evaluated the FA measures in the olfactory area without assessing the values in medulla oblongata and pontine tegmentum mainly because the data sets reported here were acquired without cardiac gating, and signals of medulla and pons were likely contaminated by physiological noises. It would be important, in future studies, to further examine the DTI signals in medulla oblongata and pontine tegmentum. We would like to further point out that previous DTI studies have observed brainstem signal abnormalities related to rapid eye movement sleep behavior disorder, which may precede parkinsonism by several years and has a high conversion rate to PD, Lewy body dementia, and multiple system atrophy (García-Lorenzo et al., 2013; Iranzo et al., 2013; Scherfler et al., 2011).

In this study, we did not observe any correlation between disease duration and FA signals measured from olfactory tract (Table 3). This appears to be consistent with findings from a previous clinical study, indicating that hyposmia is independent of disease stage and duration (Doty 2007). However, another study reported that the loss of anterior olfactory neurons correlated with disease duration (Pearce et al., 1995). The inconsistency may potentially result from the possibilities that (i) the tissue damage in the olfactory tracts occurs mainly in early PD phases, and the subsequent changes over time in later PD phases may be less pronounced; and (ii) a larger number of patients are needed to detect the correlation between olfactory FA signal abnormalities and the disease duration of PD, which is heterogeneous in nature.

As shown in Table 2, the FA values in the olfactory tract ROI are lower than those in other brain regions. Some reasons for this are the following: First, the manually drawn olfactory tract ROI was larger than the olfactory tract, mainly to account for intersubject variation in the olfactory tract location. As a result, the mean FA value calculated from the entire olfactory tract ROI was lowered by the inclusion of background voxels. Second, the olfactory tract is small, and thus it is likely that the measured FA values are affected by the partial volume effect. DWI protocols capable of producing high spatial-resolution images are thus preferred for imaging the olfactory tract. Third, the susceptibility artifact near the olfactory region is pronounced, potentially leading to reduced signal-to-noise ratio and robustness in the FA quantification.

Many clinical measures and criteria exist for the diagnosis of PD (Malek et al., 2017; Schrag et al., 2002; Yong et al., 2013). The findings from our imaging study suggest that the FA values obtained from olfactory tract, corticospinal tract, superior longitudinal fasciculus (temporal part), and cingulum (near hippocampus) provide valuable information that may be combined with the existing nonimaging measures to further improve the sensitivity, specificity, and accuracy of PD diagnosis. In addition, as shown by Menke and colleagues (2009), DTI data may be combined with other MRI contrasts to further improve the sensitivity and specificity in differentiating PD patients from controls. Specifically, T1-weighted imaging and susceptibility-weighted imaging provide information that is highly relevant to PD: (i) A recent study reported a correlation between olfactory loss and basal ganglia volumes measured with T1-weighted MRI in PD patients (Campabadal et al., 2017); and (ii) susceptibility-weighted imaging-based measurement of nigrosome can differentiate PD patients from healthy controls (Schwarz et al., 2014). Furthermore, it has been shown that brain abnormalities in early PD stages may also be detected with functional imaging of the dopamine transporter (Postuma et al., 2012; Sommer et al., 2004). Therefore, it would be worthwhile to consider a protocol that incorporates DTI and dopamine transporter imaging for early PD diagnosis.

There are some limitations in this study: First, we did not assess DTI signals in pons and medulla, which are affected in an early stage of PD and should be examined with data obtained from cardiac-gated scans. Second, without comparing with DTI data obtained from patients of other types of neurological diseases, we do not know whether the findings are specific to PD. On one hand, a recent study showed that MRI-based volumetric measures of olfactory bulb could be used to differentiate PD from multiple system atrophy (Chen et al., 2014). On the other hand, multiple neurological diseases (e.g., Alzheimer's disease, dementia with Lewy bodies, and Huntington's disease) are commonly associated with impaired sense of smell (Doty, 2017; Doty et al., 1987; Hawkes et al., 1999), and it is possible that the FA signal abnormalities in olfactory tract may also be pronounced in neurological diseases other than PD (Cross et al., 2013; Rey et al., 2018). Third, in this study we did not measure the smell function with a previously validated tool such as the University of Pennsylvania Smell Identification Test (Doty et al., 1984; Ibarretxe-Bilbao et al., 2010). Fourth, this study combined subjects from PD several stages and disease durations of PD, although differences in DTI measures have been observed in different stages and disease durations, such as in a recent DTI study of PD subjects in Hoehn and Yahr stages 1 versus 2 (Wen et al., 2016). Future studies on larger cohorts of subjects should allow for assessments of PD subjects with different stages and disease durations. Fifth, with the acquired data we were unable to calculate diffusional kurtosis, which is expected to be more sensitive than DTI in detecting PD-induced brain tissue abnormalities (Kamagata et al., 2014). Sixth, there were age differences between PD patients and healthy controls. Although a linear regression procedure was used to minimize the impact of age difference on the results, it was possible that residual artifacts (e.g., resulting from a potential nonlinear dependence of FA value on age) might exist even after regression.

Acknowledgment

This research is supported by NIH Grants R01 NS 074045 and R21 EB 018419.

Author Disclosure Statement

No competing financial interests exist.

References

Andersson JLR, Sotiropoulos SN. 2016. An integrated approach to correction for off-resonance effects and subject movement in diffusion MR imaging. Neuroimage 125:1063–1078.

Atkinson-Clement C, Pinto S, Eusebio A, Coulon O. 2017. Diffusion tensor imaging in Parkinson's disease: review and meta-analysis. Neuroimage Clin 16:98–110.

Basser PJ, Mattiello J, LeBihan D. 1994. MR diffusion tensor spectroscopy and imaging. Biophys J 66:259–267.

Braak H, Ghebremedhin E, Rüb U, et al. 2004. Stages in the development of Parkinson's disease-related pathology. Cell Tissue Res 318:121–134.

Campabadal A, Uribe C, Segura B, et al. 2017. Brain correlates of progressive olfactory loss in Parkinson's disease. Parkinsonism Relat Disord 41:44–50.

Chen N-K, Chang H-C, Bilgin A, et al. 2018. A diffusion-matched principal component analysis (DM-PCA) based two-channel denoising procedure for high-resolution diffusion-weighted MRI. PLoS One 13:e0195952.

Chen S, Tan H, Wu Z, et al. 2014. Imaging of olfactory bulb and gray matter volumes in brain areas associated with olfactory function in patients with Parkinson's disease and multiple system atrophy. Eur J Radiol 83:564–570.

Cochrane CJ, Ebmeier KP. 2013. Diffusion tensor imaging in parkinsonian syndromes: a systematic review and meta-analysis. Neurology 80:857–864.

Cousineau M, Jodoin PM, Morency FC, et al. 2017. A test–retest study on Parkinson's PPMI dataset yields statistically significant white matter fascicles. Neuroimage Clin 16:222–233.

Cross DJ, Anzai Y, Petrie EC, et al. 2013. Loss of olfactory tract integrity affects cortical metabolism in the brain and olfactory regions in aging and mild cognitive impairment. J Nucl Med 54:1278–1284.

Del Tredici K, Braak H. 2016. Review: sporadic Parkinson's disease: development and distribution of α-synuclein pathology. Neuropathol Appl Neurobiol 42:33–50.

Doty RL. 2007. Olfaction in Parkinson's disease. Parkinsonism Relat Disord 13 Suppl 3:S225–S228.

Doty RL. 2017. Olfactory dysfunction in neurodegenerative diseases: is there a common pathological substrate? Lancet Neurol 16:478–488.

Doty RL, Reyes PF, Gregor T. 1987. Presence of both odor identification and detection deficits in Alzheimer's disease. Brain Res Bull 18:597–600.

Doty RL, Shaman P, Dann M. 1984. Development of the University of Pennsylvania smell identification test: a standardized microencapsulated test of olfactory function. Physiol Behav 32:489–502.

García-Lorenzo D, Longo-Dos Santos C, Ewenczyk C, et al. 2013. The coeruleus/subcoeruleus complex in rapid eye movement sleep behaviour disorders in Parkinson's disease. Brain 136(Pt 7):2120–2129.

Georgiopoulos C, Warntjes M, Dizdar N, et al. 2017. Olfactory impairment in Parkinson's disease studied with diffusion tensor and magnetization transfer imaging. J Parkinsons Dis 7: 301–311.

Goedert M, Spillantini MG, Del Tredici K, Braak H. 2013. 100 Years of Lewy pathology. Nat Rev Neurol 9:13–24.

Hawkes CH, Shephard BC, Daniel SE. 1999. Is Parkinson's disease a primary olfactory disorder? QJM 92:473–480.

Ibarretxe-Bilbao N, Junque C, Marti M-J, et al. 2010. Olfactory impairment in Parkinson's disease and white matter abnormalities in central olfactory areas: a voxel-based diffusion tensor imaging study. Mov Disord 25:1888–1894.

Iranzo A, Tolosa E, Gelpi E, et al. 2013. Neurodegenerative disease status and post-mortem pathology in idiopathic rapid-eye-movement sleep behaviour disorder: an observational cohort study. Lancet Neurol 12:443–453.

Joshi N, Rolheiser TM, Fisk JD, et al. 2017. Lateralized microstructural changes in early-stage Parkinson's disease in anterior olfactory structures, but not in substantia nigra. J Neurol 264:1497–1505.

Kamagata K, Tomiyama H, Hatano T, et al. 2014. A preliminary diffusional kurtosis imaging study of Parkinson disease: comparison with conventional diffusion tensor imaging. Neuroradiology 56:251–258.

Kim M, Park H. 2016. Using tractography to distinguish SWEDD from Parkinson's disease patients based on connectivity. Parkinsons Dis 2016:8704910.

Malek N, Lawton MA, Grosset KA, et al. 2017. Utility of the new Movement Disorder Society clinical diagnostic criteria

for Parkinson's disease applied retrospectively in a large cohort study of recent onset cases. Parkinsonism Relat Disord 40:40–46.

Menke RA, Scholz J, Miller KL, et al. 2009. MRI characteristics of the substantia nigra in Parkinson's disease: a combined quantitative T1 and DTI study. Neuroimage 47:435–441.

Mole JP, Subramanian L, Bracht T, et al. 2016. Increased fractional anisotropy in the motor tracts of Parkinson's disease suggests compensatory neuroplasticity or selective neurodegeneration. Eur Radiol 26:3327–3335.

Pearce RK, Hawkes CH, Daniel SE. 1995. The anterior olfactory nucleus in Parkinson's disease. Mov Disord 10:283–287.

Pierpaoli C, Jezzard P, Basser PJ, et al. 1996. Diffusion tensor MR imaging of the human brain. Radiology 201:637–648.

Postuma RB, Aarsland D, Barone P, et al. 2012. Identifying prodromal Parkinson's disease: pre-motor disorders in Parkinson's disease. Mov Disord 27:617–626.

Rey NL, Wesson DW, Brundin P. 2018. The olfactory bulb as the entry site for prion-like propagation in neurodegenerative diseases. Neurobiol Dis 109(Pt B):226–248.

Rolheiser TM, Fulton HG, Good KP, et al. 2011. Diffusion tensor imaging and olfactory identification testing in early-stage Parkinson's disease. J Neurol 258:1254–1260.

Scherfler C, Frauscher B, Schocke M, et al. 2011. White and gray matter abnormalities in idiopathic rapid eye movement sleep behavior disorder: a diffusion-tensor imaging and voxel-based morphometry study. Ann Neurol 69:400–407.

Schrag A, Ben-Shlomo Y, Quinn N. 2002. How valid is the clinical diagnosis of Parkinson's disease in the community? J Neurol Neurosurg Psychiatry 73:529–534.

Schwarz ST, Abaei M, Gontu V, et al. 2013. Diffusion tensor imaging of nigral degeneration in Parkinson's disease: a region-of-interest and voxel-based study at 3 T and systematic review with meta-analysis. Neuroimage Clin 3:481–488.

Schwarz ST, Afzal M, Morgan PS, et al. 2014. The ''swallow tail'' appearance of the healthy nigrosome—a new accurate test of Parkinson's disease: a case-control and retrospective cross-sectional MRI study at 3T. PLoS One 9:e93814.

Skorpil M, Rolheiser T, Robertson H, et al. 2011. Diffusion tensor fiber tractography of the olfactory tract. Magn Reson Imaging 29:289–292.

Smith SM, Jenkinson M, Johansen-Berg H, et al. 2006. Tract-based spatial statistics: voxelwise analysis of multi-subject diffusion data. Neuroimage 31:1487–1505.

Sommer U, Hummel T, Cormann K, et al. 2004. Detection of presymptomatic Parkinson's disease: combining smell tests, transcranial sonography, and SPECT. Mov Disord 19: 1196–1202.

Wakana S, Caprihan A, Panzenboeck MM, et al. 2007. Reproducibility of quantitative tractography methods applied to cerebral white matter. Neuroimage 36:630–644.

Wen M-C, Heng HSE, Ng SYE, et al. 2016. White matter microstructural characteristics in newly diagnosed Parkinson's disease: an unbiased whole-brain study. Sci Rep 6: 35601.

Yong M-H, Allen JC, Prakash KM, Tan E-K. 2013. Differentiating non-motor symptoms in Parkinson's disease from controls and hemifacial spasm. PLoS One 8:e49596.

Address correspondence to:
Nan-Kuei Chen
Department of Biomedical Engineering
University of Arizona
1127 E. James E. Rogers Way
P.O. Box 210020
Tucson, AZ 85721-0020

E-mail: nkchen@email.arizona.edu